Astrometry of Four Binary Star Candidates

Sophia Mitchell[1], Kailash Elumalai[1], Cyrus Kuester-Ha[1], Owen Gabriel Alvarrez[1], Kalée Tock[1]

[1] Stanford Online High School, Palo Alto, California

Abstract

Images taken by LCOGT (Las Cumbres Observatory Global Telescope Network) telescopes, historical measurements, and data from Gaia space telescopes were used to investigate star systems WDS 08118-0717 GWP 994, WDS 07568+1904 TVB 179, WDS 06289+2044 SLE 750, and WDS 06386-4813 DUN 31. For system GWP 994, proper motion, parallax, velocity comparisons, and position suggest a gravitationally bound system. However, the plots based on historical data were inconclusive, suggesting that further research is needed to determine the relationship of the stars. System DUN 31 has stars which are too far apart to suggest being gravitationally bound, though they are likely to share a physical history. Systems SLE 750 and TVB 179 are both likely not bound due to velocity comparisons.

1. Introduction

The study of double stars provides a unique opportunity for professional astronomers and amateurs alike to provide measurements to a field that has only recently begun its transition to the digital age. Star systems were observed to determine whether they were physically related or not. Prior to choosing star systems, several criteria had to be met. The star systems had to have a secondary star magnitude of less than 13, a difference in (delta) magnitude of less than 3, a separation between 5 and 20 arcseconds, previous classification as a physical double, and a right ascension that allows for imaging during the month of January, when this study was conducted. These criteria were selected as we needed stars that were bright enough to be imaged by the LCOGT telescopes. Also, the stars had to have similar magnitudes, to guarantee that both can be exposed in a single frame. The separation constraint ensured that the stars were as close as feasible without being too close for the equipment used. Based on these criteria, four target star systems were chosen: WDS 06386-4813 DUN 31, WDS 08118-0717 GWP 994, WDS 06289+2044 SLE 750, and WDS 07568+1904 TVB 179.

The absolute Gaia DR3 GMAG (G-band mean magnitude) of each target was determined in two ways. First, GMAG was calculated from Gmag and parallax according to the formula:

$$Absolute\ GMAG = Gmag + 5 * (log_{10}(Parallax/1000) + 1)$$

The second way of determining absolute GMAG was to query the value directly from the Gaia DR3 Astrophysical Parameters table on VizieR. As shown in Table 1, the absolute GMAG values were similar using both methods. The slight discrepancies may arise from the incorporation of spectral data, because the GMAG column in the Astrophysical Parameters table is described as "Absolute magnitude MG from GSP Phot Aeneas best library using BP/RP spectra". The Hertzsprung-Russell diagram of Gaia Data Release 2 (GAIA Hertzsprung Russell diagram, 2018) was used to estimate the stars' masses from

absolute GMAG and the color index corresponding to magnitude in the Gaia BP-band minus magnitude in the Gaia RP-band. These mass estimates are also shown in Table 1.

Table 1. Gaia DR3 values used to estimate mass based on Gaia DR3 Hertzsprung-Russell Diagram (Babusiaux et al., 2018).

System	BP-RP Color Indices	Absolute GMAG calculated from Gmag and parallax	Absolute GMAG from Gaia DR3 Astrophysical Parameters Table	Estimated Masses
DUN 31	1.1, 0.1	-1.11, 1.63	-0.9831, 1.3505	0.95, 2.0
GWP 994	0.8, 0.9	3.74, 5.04	3.7347, 4.9704	1.0, 1.0
SLE 750	0.9, 0.9	4.00, 4.96	3.9454, 4.9202	1.1, 1.0
TVB 179	0.7, 0.7	2.73, 3.34	2.7449, 3.3619	1.1, 1.0

The Washington Double Star Catalog position angle (PA) and separation (Sep) are shown in Table 2 along with the corresponding main sequence star spectral types found in previous literature or estimated from the masses in Table 1 according to the relations in Morgan, 2023.

Table 2. WDS PA and Sep, with spectral types of the target stars.

System	PA (º)	Sep (")	Primary star spectral type	Spectral type primary star source	Secondary star spectral type	Spectral type secondary star source
DUN 31	320.7	12.9	G8III	(Cruzalèbes, P. et al., 2019)	A	(Morgan, 2023)
GWP 994	146	14.7	G5V	(Houk, Swift, 2016)	G	(Morgan, 2023)
SLE 750	224	6.8	G	(Morgan, 2023)	G	(Morgan, 2023)
TVB 179	254	5.5	G	(Morgan, 2023)	G	(Morgan, 2023)

By investigating these double stars with data from the Gaia mission (Prusti, 2016, Vallenari, 2022), the goal was to determine escape velocities, separations, proper motions, and relative proper motions (rPM) of each target. An rPM value less than 0.2 indicates that the motion is common proper motion (i.e., likely to be physically related), which helps in classifying the double star system (Harshaw, 2016). Additionally, historic data provided by the U.S. Naval Observatory is used to plot the motion of the secondary relative to the primary as a function of time, providing evidence that helps to characterize the system. Analysis of the 3D separation, mass, escape velocity, relative velocity, and distance of each star system is also used to suggest a classification for each system.

2. Equipment and Methods

The Las Cumbres Observatory Global Telescope (LCOGT) network 0.4m telescopes were used to capture images of the star system, which were then used to find the PA and Sep of the system. The telescope structure has a primary, secondary and corrector plate (Meade) with LCOGT focus mechanism driving corrector plate/secondary. The maximum slewing speed is 10 degrees/s, the blind pointing accuracy is ~30", and the mounting setup is Meade 16-inch (40cm) RCS tube and 3-element optics, mounted in LCOGT equatorial C-ring mounting. The specific telescopes used for these observations were in Cerro Tololo, Chilé, Tenerife, Spain, and Sutherland Observatory, South Africa. The measurements from each respective image are shown in Table 3.

3. Measurements

Table 3. Reduction of images including average values and standard error (S.E.)

System, Date	Image / Value	1	2	3	4	5	6	7	8	9	10	Average	S.E.
DUN 31, 2023.0582	**PA (º)**	320.71	320.89	320.58	320.57	320.96	320.71	320.84	320.81	320.52	320.97	**320.76**	**0.052**
	Sep (")	12.91	12.90	12.86	12.84	12.85	12.85	12.87	12.84	12.87	12.8	**12.86**	**0.001**
GWP 994, 2023.0191	**PA (º)**	146.19	146.21	146.27	146.23	146.24	146.26	146.21	146.26	146.28	146.17	**146.23**	**0.011**
	Sep (")	14.73	14.67	14.72	14.72	14.72	14.71	14.68	14.69	14.71	14.71	**14.71**	**0.006**
SLE 750, 2023.0288	**PA (º)**	224.58	224.76	224.66	224.55	224.7	224.59	224.34	224.56	224.34	224.42	**224.55**	**0.144**
	Sep (")	6.66	6.78	6.78	6.75	6.76	6.77	6.75	6.78	6.77	6.76	**6.76**	**0.036**
TVB 179, 2023.0315	**PA (º)**	255.14	254.23	254.47	254.13	254.16	254.82	255.04	254.65	254.51	254.12	**254.53**	**0.011**
	Sep (")	5.51	5.55	5.54	5.56	5.42	5.45	5.53	5.47	5.48	5.63	**5.51**	**0.019**

The process employed to find the PA and Sep from each image in AstroImageJ is shown in Figure 1. Each set of images was clearly resolved, and the PA and Sep measurement averages matched previously recorded data.

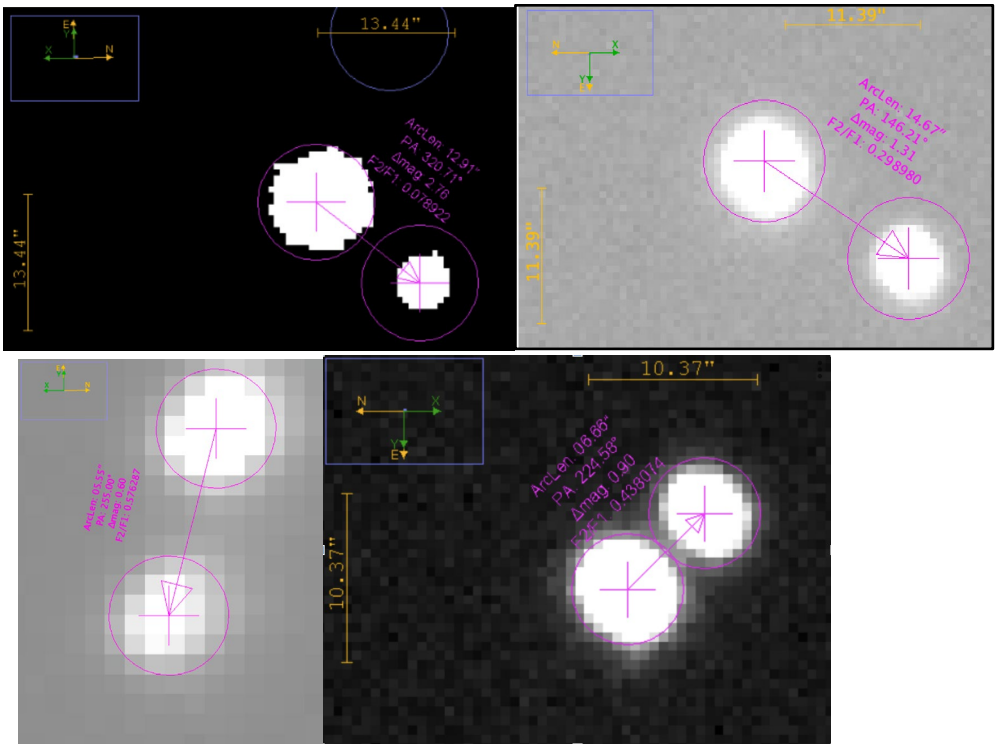

Figure 1: AstroImageJ analyses of images clockwise starting from top left: WDS 06386-4813 DUN 31, WDS 08118-0717 GWP 994, WDS 06289+2044 SLE 750, and WDS 07568+1904 TVB 179

4. Discussion

The Gaia proper motion and parallax measurements shown in Table 4 were used in conjunction with the image measurements of the previous section to conduct an analysis of each system. The rPM metric is defined as the difference vector of the stars proper motions divided by the longer of the two proper motion vectors in accordance with Harshaw, 2016. As noted above, an rPM less than 0.2 indicates a common proper motion system.

Table 4. Proper motion and parallax measurements from GAIA data.

System	Parallax of Primary (mas)	Parallax of Secondary (mas)	Proper Motion of Primary RA (mas/yr)	Proper Motion of Primary Dec (mas/yr)	Proper Motion of Secondary RA (mas/yr)	Proper Motion of Secondary Dec (mas/yr)	rPM
DUN 31	6.65 ± 0.08	6.74 ± 0.03	4.0 ± 0.11	19.7 ± 0.12	5.5 ± 0.04	18.8 ± 0.04	0.087
GWP 994	7.84 ± 0.02	7.84 ± 0.02	-99.0 ± 0.02	7.4 ± 0.02	-99.3 ± 0.02	7.8 ± 0.02	0.005

SLE 750	2.72 ± 0.02	2.76 ± 0.01	0.5 ± 0.02	-10.6 ± 0.01	0.7 ± 0.02	-10.6 ± 0.01	0.019
TVB 179	1.77 ± 0.02	1.76 ± 0.01	-13.5 ± 0.02	-19.3 ± 0.01	-13.5 ± 0.01	-19.4 ± 0.01	0.004

Based on past measurements of the star system, historical relative motion plots were created by converting the measured PA and Sep, where the PA was given in radians, into RA and Dec in arcseconds using the formulas given below:

$$RA = x_{coordinate} = Sep * sin(PA)$$
$$Dec = y_{coordinate} = -Sep * cos(PA)$$

Each measurement was then plotted to create the graphs shown in Figure 2. These graphs were evaluated to determine whether there was a consistent curve/pattern in the plot, which would suggest motion of the secondary star around the primary star.

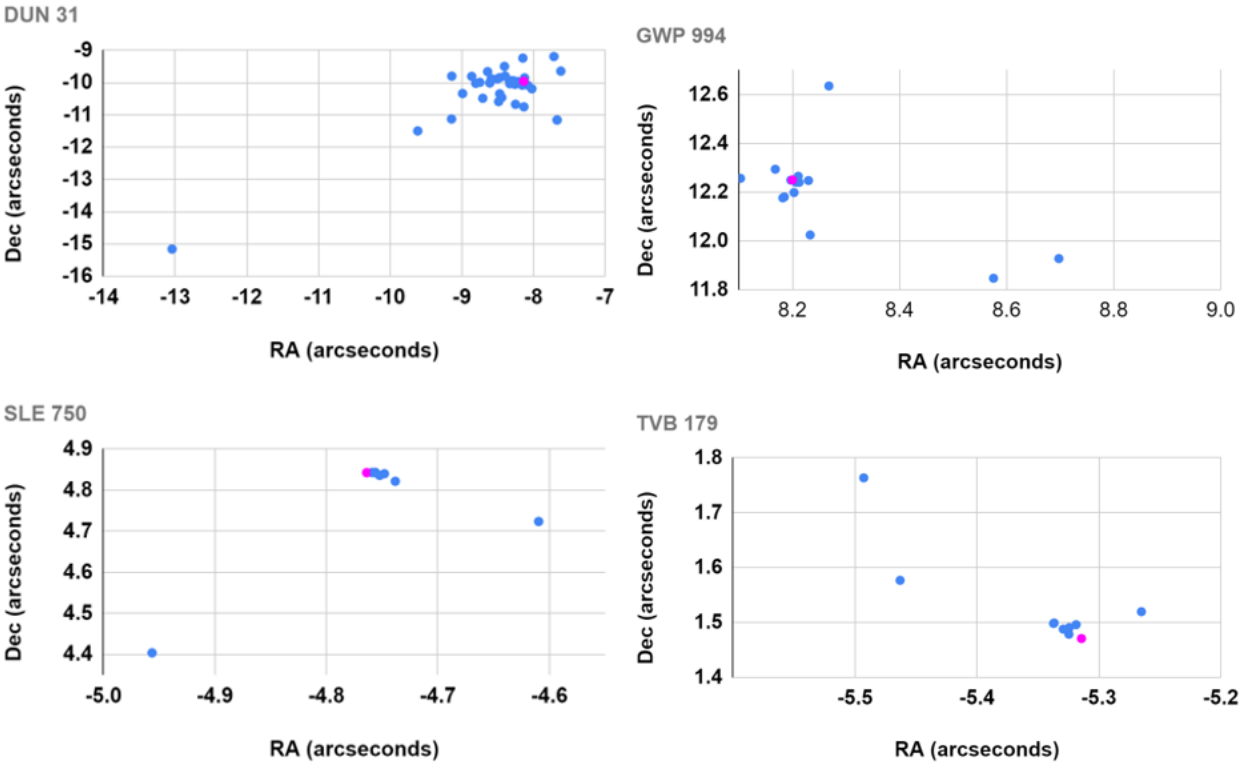

Figure 2: Scatter plots of each star system's historical RA and Dec measurements and the next measurement's predicted region.

For DUN 31, although the outlier points are due to great distance in time from earlier observations, which were taken over a large time span, modern observations form the clump of points around (-8.5, -10) and show a more consistent grouping. Considering these points and the time span over which these measurements were made, there is no evidence to suggest the secondary star is moving around the primary

star, as the cluster is easily explained by small deviations. Our measurement, made using LCOGT images, is in the middle of the clump.

For GWP 994, the outlier points were taken over the past 100-120 years, whereas observations from the past 20 years that form the clump of points around (8.2 arcseconds, 12.2 arcseconds) show a more consistent grouping. Thus, there is no evidence to suggest the secondary star is moving around the primary star. Based on the clump, our measurement is located as part of a general clump of stars in the left-hand corner of the plot. Interestingly, the Gaia DR3 point is at (6.57 arcseconds, 12.09 arcseconds) rather than within the main clump.

Similarly, for SLE 750, the more modern points form the clump, which does not suggest any motion of the secondary around the primary. Our image measurement is close to the clump of recent points.

For TVB 179, the more recent observations once again compose a clump rather than showing a clear pattern of motion. Our measurement using LCOGT images is located just below a cluster of measurements mostly consisting of recent observations.

We then performed analysis of the relative velocities of the systems to conclude their likelihood of being gravitationally bound, as shown in Table 5. Note that the masses in Table 5 are given as multiples of 10^{30} kg, *not* as solar masses, for the units to be consistent with the Universal Gravitation constant G in the equation for escape velocity. Also note that the radial velocities from are given in units of m/s in Gaia DR3, so these are multiplied by 1000 to transform them into units of m/s for consistency with G.

Table 5. Analysis of velocity calculations for each star system.

Name	Expression	DUN 31	GWP 994	SLE 750	TVB 179
Mass of primary star * **10^{30} (kg)**	m_1	1.9	2.0	2.2	2.2
Mass of secondary star * **10^{30} (kg)**	m_2	4.0	2.0	2.0	2.0
Spatial separation (m)	r	6.2E16	2.8E14	1.0E16	9.9E16
Escape velocity (m/s)	$\sqrt{\frac{2G(m_1+m_2)}{r}}$	112.7	1380.4	236.7	75.2
Relative proper motion vector	$\sqrt{(pm_{RA1}-pm_{RA2})^2+(pm_{dec1}-pm_{dec2})^2}$	1.7	0.5	0.2	0.1
Parallax primary (mas)	plx	6.65	7.8	2.72	1.77
Relative transverse velocity (m/s)	$\frac{4740*(relative\ proper\ motion\ vector)}{plx}$	1211.7	303.8	348.5	267.8
Relative radial velocity (m/s)	*(radial velocity$_1$ - radial velocity$_2$)1000*	1650.0	330.0	4620.0	490.0

Relative 3D space velocity (m/s)	$\sqrt{relative\ radial^2 + relative\ transverse^2}$	2047.1	448.5	4633.1	558.4

For DUN 31, although the stars are moving together through space, they are too far apart to be gravitationally bound. Even though the rPM from Table 4 indicates the stars are moving together, they are around 30.5 pc away from each other, and the escape velocity of the system is too low compared to the relative velocities of the stars for them to be a binary system.

For GWP 994, it is likely that the stars are gravitationally bound. The rPM is much less than 0.02, indicating common proper motion (CPM). Additionally, the stars have a negligible distance and a very high escape velocity compared to the transverse velocity, radial velocity, and relative 3D space velocity. However, the data plot does not suggest the secondary star is in motion around the primary star, at least not with an observable orbit, as the period of orbit seems to be very high. Ideally, more data should be collected.

For SLE 750, the results do not suggest the stars are gravitationally bound. The rPM is almost exactly 0.02, which can suggest CPM, it has very high relative velocities compared to the escape velocity.

For TVB 179, it is not likely that the stars are gravitationally bound. Even though the rPM has a value less than 0.02, the relative velocities are larger than the escape velocities. Analysis of historical data was inconclusive, suggesting that further research should be collected to come to a complete conclusion.

5. Conclusions

Each star system had separate conclusions based on the data above. Three star systems are most likely not bound, and one has been firmly decided as gravitationally bound. DUN 31 is most likely not gravitationally bound due to the stars being too far apart, GWP 994 is probably bound due to the comparison of escape and relative velocity and rPM, SLE 750 is most likely not bound due to the velocity comparisons, and TVB 179 is also not likely to be bound due to similar reasons as SLE 750. Historical data plots did not suggest orbits for any star systems, suggesting further observation of the star systems is required.

Acknowledgements

This research was made possible by the Washington Double Star catalog maintained by the U.S. Naval Observatory, the Stelledoppie catalog maintained by Gianluca Sordiglioni, Astrometry.net, and AstroImageJ software which was written by Karen Collins and John Kielkopf.

This work has also made use of data from the European Space Agency (ESA) mission Gaia (https://www.cosmos.esa.int/gaia), processed by the Gaia Data Processing and Analysis Consortium (DPAC, https://www.cosmos.esa.int/web/gaia/dpac/consortium). Funding for the DPAC has been provided by national institutions, in particular the institutions participating in the Gaia Multilateral Agreement.

This work makes use of observations taken by the 0.4m telescopes of Las Cumbres Observatory Global Telescope Network located in Cerro Tololo, Chilé, Tenerife, Spain, and Sutherland Observatory, South Africa.

The team would like to thank Thomas Smith for his thorough and thoughtful review of this paper.

References

Cruzalèbes, P. et al. (2019). A catalogue of stellar diameters and fluxes for mid-infrared interferometry, Monthly Notices of the Royal Astronomical Society, 490(3), 3158–3176. https://doi.org/10.1093/mnras/stz2803

Hou, N. & Swift, C. (1999). Michigan catalogue of two-dimensional spectral types for the HD Stars, Vol. 5. Michigan Spectral Survey, Ann Arbor, Dep. Astron., Univ. Michigan, Vol. 5, p. 0. Retrieved from http://cdsarc.u-strasbg.fr/viz-bin/cat/III/214.

Harshaw, R. (2016). CCD Measurements of 141 Proper Motion Stars: The Autumn 2015 Observing Program at the Brilliant Sky Observatory, Part 3. Journal of Double Star Observations, 12 (4), 394 - 399. Retrieved from http://www.jdso.org/volume12/number4/Harshaw_394_399.pdf.

Gaia Collaboration, C. Babusiaux, F. Van Leeuwen, et al. (2018) Gaia Data Release 2: Observational Hertzspring-Russell diagrams. A&A 616, A10.

Gaia Collaboration, T. Prusti, J.H.J. de Bruijne, et al. (2016b) The Gaia mission. A&A 595, A1.

Gaia Collaboration, A. Vallenari, A. G. A. Brown, et al. (2022k) Gaia Data Release 3: Summary of the content and survey properties. arXiv e-prints, pp. arXiv:2208.00211.

Morgan, Siobahn (2023). Spectral Type Characteristics. Retrieved Jan, 2023 from https://sites.uni.edu/morgans/astro/course/Notes/section2/spectralmasses.html

GAIA Hertzsprung Russell diagram, 2018 https://www.esa.int/ESA_Multimedia/Images/2018/04/Gaia_s_Hertzsprung-Russell_diagram